

Effect of WC particle size on Co distribution in liquid-phase-sintered functionally graded WC–Co composite

Peng Fan, Oladapo O. Eso, Zhigang Zak Fang^{*}, H.Y. Sohn

Department of Metallurgical Engineering, University of Utah, Salt Lake City, UT 84112, USA

Received 20 December 2006; accepted 5 February 2007

Abstract

Functionally graded WC–Co materials can be manufactured by controlling liquid phase migration or liquid redistribution during liquid phase sintering. The driving force of liquid phase migration is liquid migration pressure P_m which depends on the solid particle size d and the liquid phase volume fraction u . In this study, the effect of d on P_m has been studied experimentally for WC–Co system. The results show that P_m is proportional to $1/d^{0.4}$ which is different from previous postulation that P_m is proportional to $1/d$. The reason for this difference is that the previous postulation was based on the assumption that all the solid particles in a composite are mono-sized and isometric-shaped, while in real WC–Co composites WC particles usually have non-isometric shape and there is a wide particle size distribution. The dependence of P_m on both d and u has been quantitatively established, enabling the prediction of final Co composition gradient in liquid-phase-sintered WC–Co composites.

© 2007 Elsevier Ltd. All rights reserved.

Keywords: Liquid phase sintering; Cemented carbide; Functionally graded materials; Liquid redistribution; Composition gradient

1. Introduction

Functionally graded cemented tungsten carbide (WC–Co) is a typical example of how the performance of engineering components can be improved by fabricating the material with a compositional gradient. For example, a WC–Co material with cobalt content increasing from surface to the interior of the bulk of the material would have a good combination of wear resistance and fracture toughness. However, the manufacture of WC–Co with graded cobalt compositions is a difficult challenge, because the cobalt phase will migrate during liquid phase sintering, which results in a homogeneous cobalt distribution within the material. It is known that during liquid phase sintering liquid phase tends to flow from a region with a higher liquid volume fraction and/or larger solid particles to a

region with a lower liquid volume fraction and/or smaller solid particles [1–6]. This phenomenon of the redistribution of the liquid phase within the composite materials has been termed liquid phase migration (LPM), and the driving force of LPM is termed liquid migration pressure, P_m [1,2]. During liquid phase sintering, if P_m is initially inhomogeneous within a composite material, the liquid phase will flow from a region of low P_m to a region of high P_m . In other words, the liquid migration pressure may also be called imbibition pressure, according to its physical effect. However, the term “liquid migration pressure” is used in this article to be consistent with the convention of this field. Liquid phase migration or liquid phase redistribution does not stop until P_m reaches homogeneity everywhere within the entire composite material.

Conceptually, it is widely recognized that the equilibrium distribution of liquid or the final composition gradient is determined by liquid migration pressure, which depends on liquid volume fraction, solid particle size, and other microstructural factors. Quantitatively, there have

^{*} Corresponding author. Tel.: +1 801 414 3251.

E-mail address: Zhigang.Fang@mines.utah.edu (Z.Z. Fang).

also been a number of published efforts on modeling the dependence of the liquid migration pressure on these primary factors. However, none of the reported models to date agrees satisfactorily with the experimental data. The dependence of liquid migration pressure on average particle size in particular is still uncertain. In this study, the effect of solid particle size on liquid migration pressure was studied for the WC–Co system, through experimentally examining the variation of the equilibrium liquid Co partition between the two layers of liquid-phase-sintered WC–Co bi-layers, with each layer having different WC particle sizes. Based on the experimental results, the dependence of liquid migration pressure as a function of both solid particle size and liquid volume fraction has been established, enabling the prediction of the final Co gradient in WC–Co system.

2. Models of the dependence of liquid migration pressure on particle size and volume fraction

Fundamentally the driving force of liquid phase migration or liquid phase redistribution is attributed to the reduction of the total interfacial energy of the system [4–6]. Beere [4], Park and Yoon [5] and Delannay et al. [6] theoretically modeled the variation of total interfacial free energy, F , as a function of four factors: liquid volume fraction (u), solid particle size (d), interfacial energies of solid–solid and solid–liquid interfaces (γ_{ss} and γ_{sl}), and particle coordination (n_c). The driving force of liquid phase migration, dF/dV_l (where V_l is liquid volume) was termed “spherizing force” by Park and Yoon [5], but liquid migration pressure by Lisovsky [1,2]. Throughout this paper, the term “liquid migration pressure”, or P_m , will be used to denote the driving force of liquid phase migration, since it is logically relevant with liquid phase migration. Delannay et al. [6] derived an analytical expression describing the variation of liquid migration pressure as a function of u , d , γ_{ss} , γ_{sl} , and n_c . The derivation was based on major assumptions, including that the material is an ideal composite system with mono-sized solid particles with the isometric shape and uniformly distributed in a liquid phase matrix. Unfortunately these assumptions are grossly different from real material systems where particles are neither uniform in size nor isometric in shape. There is also a lack of experimental evidence for these models. Although it may be possible, at least in principle, to quantitatively predict liquid migration pressure for various real systems by modifying these theoretical models by taking into account the distributions in particle size and shape within the real systems, the mathematical complexity and difficulty are expected to be too large to be feasible. Therefore, the only practical way to obtain the quantitative relationship between the liquid migration pressure and the microstructure factors is to establish it experimentally.

For ideal composite systems with mono-sized and isometric-shaped solid particles, liquid migration pressure depends on the following five parameters, i.e., u , d , γ_{ss} ,

γ_{sl} , and n_c according to theoretical analysis by Delannay et al. [6]. For real systems, the shape of particles and the particle size distribution also affect the liquid migration pressure. For any given real system, e.g., WC–Co, it can be assumed that the interfacial energies (γ_{ss} and γ_{sl}) and the shape and the size distribution of the particles are constant. The average coordination number (n_c) depends on liquid volume fraction (u) and particle size (d). Thus the number of the independent variables that determines the liquid migration pressure of a system is reduced to 2: the liquid volume fraction and the average particle size. The effects of other parameters are implicitly taken into account in the experimentally determined dependence of liquid migration pressure as a function of liquid volume fraction and particle size.

Lisovsky [1,2,7,8] experimentally studied the variation of liquid migration pressure, P_m , as a function of liquid volume fraction, u , for the WC–Co system. The liquid migration pressures of WC–Co samples with various Co contents were determined by measuring the radius of liquid Co surface filled in a V-shaped capillary, and the following empirical equation was obtained:

$$P_m = k_0[(1/u - 1)^{1/3} - 1.41u]/d \quad (1)$$

where P_m is the liquid migration pressure, k_0 is a coefficient, u is liquid volume fraction, and d is solid particle diameter. According to Eq. (1), P_m is predicted to diminish when $u = 0.61$, which agrees with the experimental data of the variation of P_m with u for WC–Co system [7,8]. However, as pointed out by Suresh and Mortensen [9], the agreement of Eq. (1) with experiments featuring simultaneous variations in particle size and liquid volume fraction is poor. In a recent study by the present authors [10], it was also found that Eq. (1) has a poor agreement with experimental data with respect to the variation of P_m with solid particle size, d . It was shown that the discrepancy between the experimental value and the predicted cobalt content could be as much as 100%. Needless to say, an improved model with better accuracy is needed if the materials are to be designed and manufactured with a minimum amount of experiments.

In Eq. (1), because the dependence of P_m on u (i.e., $P_m \propto [(1/u - 1)^{1/3} - 1.41u]$) was experimentally established over a wide range of u in Ref. [2], the relationship between P_m and u is considered satisfactory. The discrepancy between Eq. (1) and experiments is attributed to the assumption of the linear relationship between P_m and $1/d$. This assumption may be valid in ideal composite systems in which mono-sized and isometric-shaped solid particles are uniformly distributed in a liquid phase matrix, while in real WC–Co composite materials there is a wide distribution in WC size, and WC particles are usually non-isometric in shape.

In order to determine the correct dependence of the liquid migration pressure P_m on particle size d , we propose a non-linear relationship between P_m and $1/d$, i.e., $P_m \propto 1/$

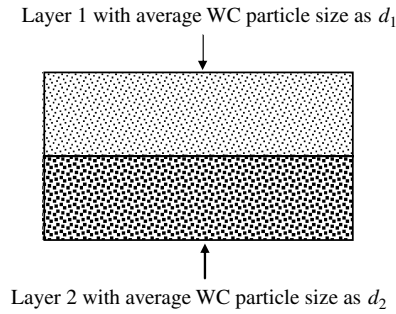


Fig. 1. Schematic of WC–Co bi-layer.

d^n , where n is a positive number. Thus, Eq. (1) is modified to be as follows:

$$P_m = k'_0[(1/u - 1)^{1/3} - 1.41u]/d^n, \quad (2)$$

where k'_0 is a coefficient. In order to determine exact values of n , consider a bi-layer configuration of a WC–Co specimen as shown in Fig. 1. The bi-layer is designed such that the WC particle size in one layer is different from that in the other layer, i.e., $d_1 \neq d_2$. Subscripts 1 and 2 denote Layers 1 and 2, respectively. If the equilibrium liquid distribution is reached in the liquid-phase-sintered WC–Co bi-layer specimen, the liquid migration pressures in the two layers will equalize, i.e., $(P_m)_1 = (P_m)_2$, which results in the following equation based on Eq. (2):

$$[(1/u_1 - 1)^{1/3} - 1.41u_1]/d_1^n = [(1/u_2 - 1)^{1/3} - 1.41u_2]/d_2^n. \quad (3)$$

Rearranging Eq. (3) leads to

$$n = \frac{\ln\{[(1/u_2 - 1)^{1/3} - 1.41u_2]/[(1/u_1 - 1)^{1/3} - 1.41u_1]\}}{\ln(d_2/d_1)}. \quad (4)$$

Using Eq. (4), n can be obtained by measuring liquid Co volume fractions and WC particle sizes in each of the two layers of a bi-layer WC–Co sample after equilibrium

liquid distribution is reached. This equation serves as a theoretical model for us to investigate the dependence of P_m on d , by conducting liquid phase sintering experiments of bi-layer WC–Co materials.

3. Experimental

WC and Co powders used in this study were supplied by Kennametal. Four types of WC powders were used, with average particle sizes of 0.8, 2.5, 5, and 20 μm , respectively. The average particle size of Co powder was approximately 1 μm . WC and Co powders were mixed together with 2% paraffin wax, and then the powder mixture was milled in heptane in a Nalgene bottle containing WC balls for fourteen hours on a rolling mill. After milling, the powder mixture was dried in a rotary evaporator at 80 $^\circ\text{C}$, and then compacted at 200 MPa into bi-layer disk-shaped samples, with each layer having different WC particle sizes and varying Co contents, except for Test Runs # G and # J, where 10%Co was used for both layers. The disk-shaped bi-layer samples were dewaxed at 300 $^\circ\text{C}$ before sintering.

Liquid phase sintering experiments were carried out in a vacuum furnace. WC–Co bi-layer samples were heated up at a rate of 10 $^\circ\text{C}/\text{min}$ to 1400 $^\circ\text{C}$, held at that temperature for 1 h, and then cooled down in the furnace by switching off the power. The liquid-phase-sintered bi-layer samples were polished and etched with Murakami's reagent. The Co contents in each layer of the WC–Co bi-layer samples were measured using energy dispersive spectroscopy (EDS) incorporated with the scanning electron microscope (SEM), with the variation of the measurements being less than 5% of the measured Co contents. The measured Co contents were then normalized so that the sum of the final Co contents in the two layers was equal to the sum of the initial Co contents in the two layers, based on the assumption of mass conservation of Co. WC particle size, d , was represented by the mean linear intercept length measured on SEM photos of the sintered samples. The variation of the grain size measurements is less than 7% of the measured

Table 1
Initial and final WC sizes and Co contents in WC–Co bi-layers

Test number	Initial				Final						n
	WC size and Co content in layer 1		WC size and Co content in layer 2		WC size, Co content and liquid volume fraction in layer 1			WC size, Co content and liquid volume fraction in layer 2			
	d (μm)	Co (%)	d (μm)	Co (%)	d (μm)	Co (%)	u	d (μm)	Co (%)	u	
A	0.8	20.0	5.0	10.0	1.1	17.7	0.38	2.4	12.3	0.27	0.56
B	0.8	10.0	5.0	20.0	1.1	17.4	0.37	2.4	12.6	0.28	0.48
C	0.8	6.0	5.0	10.0	1.1	9.8	0.22	2.4	6.2	0.15	0.37
D	0.8	10.0	5.0	6.0	1.1	9.3	0.21	2.4	6.7	0.16	0.26
E	0.8	10.0	2.5	20.0	1.1	15.6	0.34	1.6	14.4	0.32	0.25
F	0.8	20.0	2.5	10.0	1.1	15.8	0.34	1.6	14.2	0.31	0.34
G	0.8	10.0	5.0	10.0	1.1	11.8	0.27	2.4	8.2	0.19	0.35
H	0.8	6.0	5.0	10.0	1.1	10.5	0.24	2.4	5.5	0.13	0.52
I	0.8	20.0	5.0	10.0	1.1	18.4	0.39	2.4	11.6	0.26	0.69
J	0.8	10.0	20	10.0	1.1	13.6	0.30	7.5	7.4	0.17	0.25

Average $n = 0.4$.

values. The initial and final WC particle sizes and Co contents are listed in Table 1.

Liquid volume fractions of each layer of the bi-layer samples were calculated from the Co content by weight as given in Table 1. The composition of liquid Co was determined from the isothermal section of ternary Co–WC phase diagram at 1400 °C [11]. The molar volume of liquid Co was calculated from the reported dependence of the molar volume of liquid Co as a function of the composition and temperature [12] and the molar volume of WC was obtained from the same paper [12]. The obtained values of liquid volume fractions are also listed in Table 1.

4. Results

4.1. Sintering time for achieving equilibrium distribution

Since the model given by Eq. (2) is for equilibrium conditions, the specimens to be used for measurements of data must be sintered and prepared to have equilibrium liquid distribution. To meet that requirement, we must first determine the sintering conditions that will ensure the specimens are at equilibrium conditions. So, specifically, we need to determine the sintering time that is required for the specimen to reach equilibrium.

To do so, three pairs of tests, *A* and *B*, *C* and *D*, and *E* and *F*, were conducted. Each pair of specimens was prepared to have the same initial grain sizes, but a reversed initial cobalt gradient in the bi-layers. Based on experience, the specimens were sintered for one hour at 1400 °C. During sintering, cobalt is expected to migrate from the layer with lower liquid migration pressure to the layer with higher liquid migration pressure. When equilibrium conditions are reached, each pair should reach the same final cobalt distribution regardless the initial conditions, or the direction of Co migration.

In Fig. 2, the final Co distributions (solid lines) in the three pairs of specimens are displayed with the initial Co distributions (dotted lines). For example, the A0 and A1 lines denote the initial and the final Co distributions in Test A, respectively. The good agreements between the A1 and B1, C1 and D1, and E1 and F1 lines demonstrate that equilibrium liquid distributions were reached in all these tests. In other words, sintering at 1400 °C for one hour is sufficient for generating a specimen at equilibrium conditions that can be used for measuring data to be used to establish the dependence of liquid migration pressure on WC particle size.

4.2. Dependence of P_m as a function of d and u

Using the experimental procedures and the measurement techniques described earlier, the measured cobalt distribution and grain sizes of the sintered specimens are tabulated in Table 1. According to Eq. (4), the value of n was calculated from the measured d_1 , d_2 , u_1 , and u_2 for all tests, as listed in Table 1. The obtained values of n were

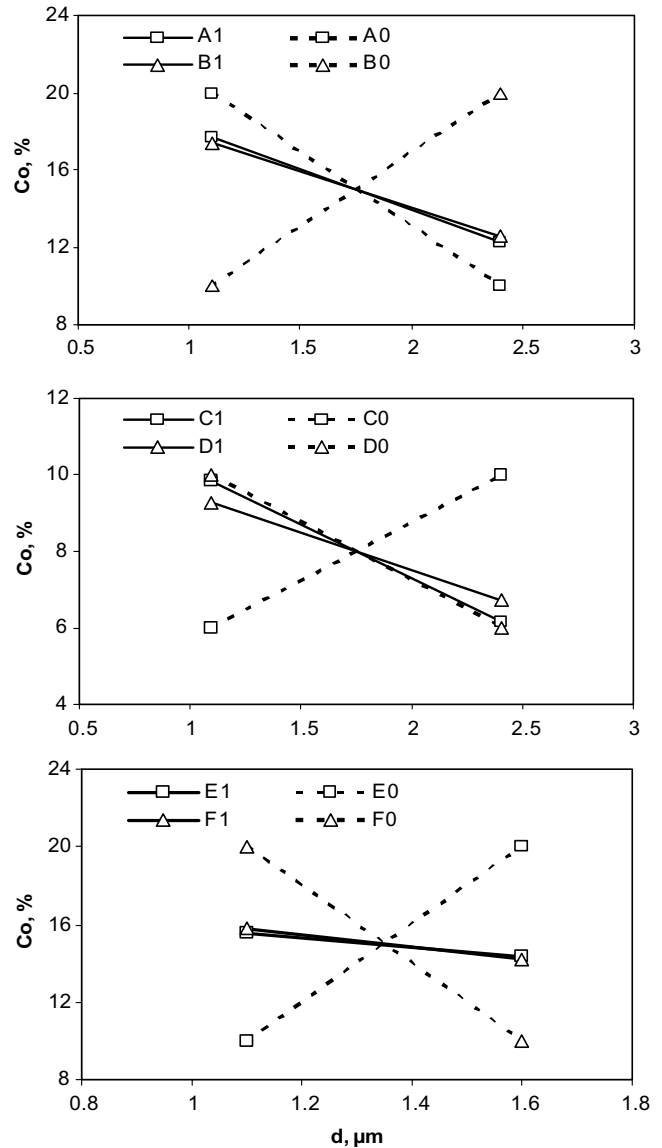


Fig. 2. Confirmation of equilibrium liquid distribution by checking agreement between the final Co gradient created by Co migrating from the layer with finer WC to the layer with coarser WC and that created by Co migrating from the layer with coarser WC to the layer with finer WC.

found to vary in the range of 0.25–0.69, and the average value of n is 0.4, suggesting that $P_m \propto 1/d^{0.4}$. The scatter for the experimentally determined n values may be attributed to the variations in measuring Co content and WC particle size, noting that there were 5% and 7% of relative errors in measuring Co content and WC particle size, respectively, as mentioned in Section 3. For example, evaluating the influence of errors in measuring Co content and WC particle size on the scatter of n for the test run # C with measured $n = 0.37$ indicates that the value of n can vary between 0.24 and 0.55, corresponding to the maximum relative errors in measuring Co content and WC particle size.

Introducing $n = 0.4$ into Eq. (2) leads to

$$P_m = k'_0 [(1/u - 1)^{1/3} - 1.41u]/d^{0.4}. \quad (5)$$

To evaluate the value of k'_0 , the liquid migration pressure needs to be measured, which, however, cannot be done directly for the bi-layer sintering in this study. Therefore, the data of liquid migration pressure in Ref. [2] for the WC–Co system with a fixed WC particle size ($d = 2.3 \mu\text{m} = 2.3 \times 10^{-6} \text{m}$) were employed to evaluate k'_0 using the following procedure.

The best fitting of the reported data in Ref. [2] leads to

$$P_m = 0.3687 \times 10^6 [(1/u - 1)^{1/3} - 1.41u]. \quad (6)$$

Comparing Eq. (5) (applicable for any WC particle size) and Eq. (6) (applicable only for one fixed WC particle size, i.e., $d = 2.3 \mu\text{m} = 2.3 \times 10^{-6} \text{m}$) leads to $k'_0/d^{0.4} = k'_0/(2.3 \times 10^{-6})^{0.4} = 0.3687 \times 10^6$.

Thus, the value of k'_0 was obtained as:

$$k'_0 = 0.3687 \times 10^6 \times (2.3 \times 10^{-6})^{0.4} = 2048.$$

Therefore, the dependence of liquid migration pressure as a function of WC particle size and the volume fraction of liquid Co phase can be expressed as:

$$P_m = 2048 [(1/u - 1)^{1/3} - 1.41u]/d^{0.4}, \quad (7)$$

where P_m is the liquid migration pressure, Pa; u is volume fraction of liquid Co phase; and d is WC particle size (i.e., the average linear intercept length), m.

5. Discussion

5.1. Design of Co gradient by controlling WC particle size

The establishment of the dependence of liquid migration pressure as a function of the volume fraction of the liquid Co phase and the WC particle size is valuable for the design and manufacture of functionally graded WC–Co composite materials.

As mentioned in Section 2, the equilibrium liquid distribution is reached only when the liquid migration pressure is uniform throughout the composite material. For any given value of liquid migration pressure, the volume fraction of liquid Co phase varies with WC particle size. A desired Co gradient can be acquired by pre-designing a suitable gradient of WC particle size. This approach can be readily used to design various bi-layer, multi-layer, or continuously graded structures of WC–Co. Two examples are given below to demonstrate how Eq. (7) can be used to design graded WC–Co structures.

The first example is to select WC particle sizes so as to obtain a desired Co gradient. Suppose that a WC–Co bi-layer structure is desired with the two layers having volume fractions of liquid Co phase to be $u_1 = 0.2$ and $u_2 = 0.1$, respectively, and the WC particle size in the first layer having been chosen to be $d_1 = 1 \mu\text{m}$. We need to select the WC particle size that should be used in the second layer to obtain the required final Co distribution. According to $(P_m)_1 = (P_m)_2$ and Eq. (7), we have

$$[(1/u_1 - 1)^{1/3} - 1.41u_1]/d_1^{0.4} = [(1/u_2 - 1)^{1/3} - 1.41u_2]/d_2^{0.4}. \quad (8)$$

Solving Eq. (8) with available values of d_1 , u_1 , and u_2 leads to $d_2 = 2.7 \mu\text{m}$, which is the WC particle size that should be used for the second layer.

The second example is to prevent liquid-redistribution-induced distortion by selecting correct Co contents in green parts intended for liquid-phase-sintered WC–Co bi-layer structures. Supposing that d_1 , d_2 and u_1 have been predetermined, a suitable value of u_2 can be obtained from solving Eq. (8). By preparing the bi-layer green parts using the selected grain sizes and the Co contents in each layer, liquid redistribution will not occur during liquid phase sintering and consequently the distortion of the sintered parts will be minimized.

To further illustrate the utility of Eq. (7), contour plots of P_m as a function of the volume fraction of liquid Co phase and WC particle size have been computed based on Eq. (7) and plotted in Fig. 3a. By converting the volume fraction of the liquid Co phase into the corresponding Co content based on molar volumes of WC and the liquid Co phase, the contour plot of P_m as a function of the Co content and WC particle size has also been computed and plotted in Fig. 3b. Any two points on the same contour line have the same liquid migration pressure and thus can represent the final or equilibrium compositions and particle sizes in a bi-layer WC–Co structure. Therefore, these contour line plots can be used to design and fabricate various graded WC–Co composite materials with bi-layer, multi-layer, or continuously graded compositions and particle sizes.

5.2. The value of n

Although $n = 1$ has been suggested by all previous theoretical models [1,2,4–6], the experimental results of this study indicate that $n = 0.4$ for the real WC–Co system. Logically the significant difference in the value of n between a real system and a model system is attributed to the fact that there is a wide distribution of particle size and particle shape in the real system, while the model is based on systems with mono-sized and isometric-shaped particles. In the following paragraph, we will demonstrate that there is indeed a significant effect of particle size distribution on the value of n .

Let us consider a liquid-phase-sintered WC–Co bi-layer consisting of Layer A and Layer B. Suppose that particle size distribution of WC in each layer is log-normal distribution as often observed for sintered WC–Co system [13], then the probability density or frequency functions of particle sizes in each layer are:

$$f(d_i, d_A, \sigma_A) = \frac{1}{\ln \sigma_A \sqrt{2\pi}} \exp \left(-\frac{(\ln d_i - \ln d_A)^2}{2 \ln^2 \sigma_A} \right) \quad (9)$$

and

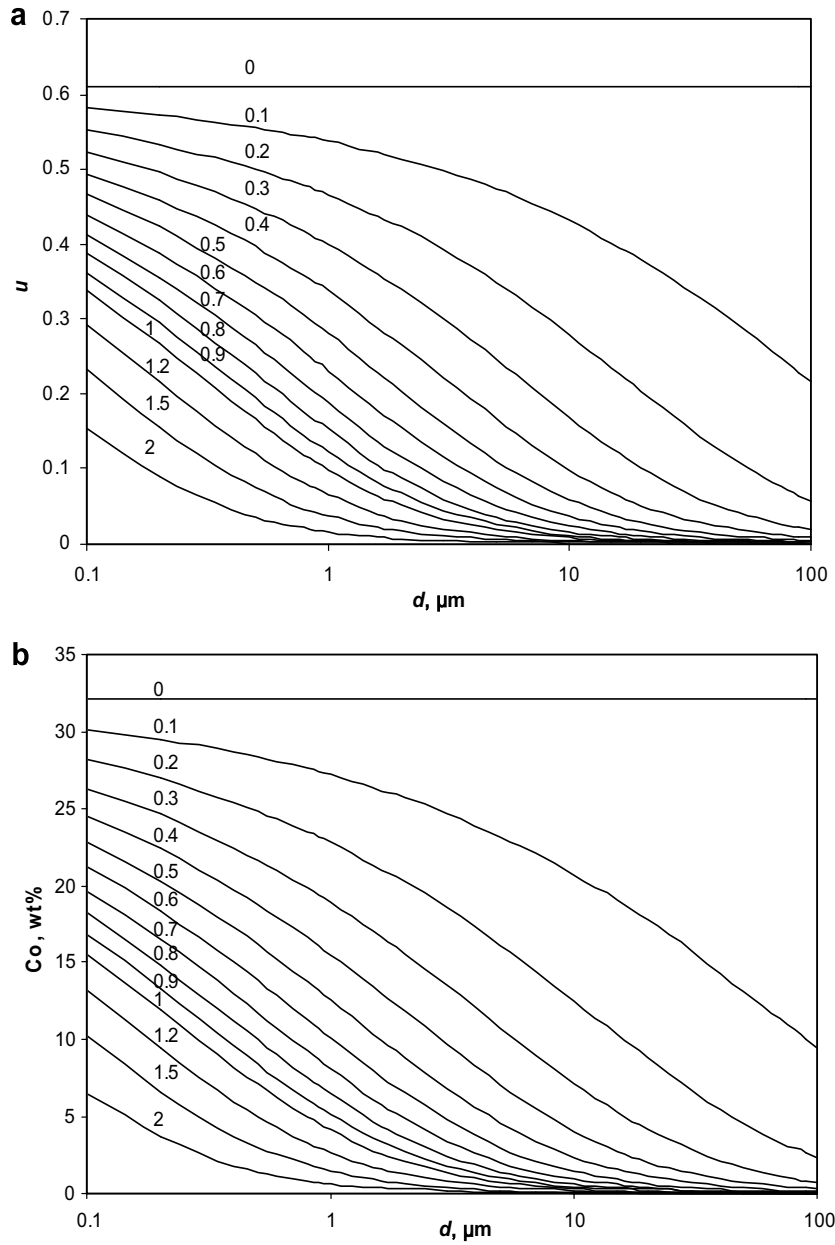


Fig. 3. Liquid migration pressure (P_m) contour. (a) As a function of volume fraction of liquid Co phase (u) and WC particle size (d). (b) As a function of Co content and WC particle size. Each line represents one iso- P_m line calculated from Eq. (7), with the number near the line indicating the corresponding P_m value in MPa.

$$f(d_i, d_B, \sigma_B) = \frac{1}{\ln \sigma_B \sqrt{2\pi}} \exp\left(-\frac{(\ln d_j - \ln d_B)^2}{2 \ln^2 \sigma_B}\right), \quad (10)$$

respectively; where d_i and d_j are an arbitrary particle size in Layers A and B, respectively; d_A and d_B are the median particle size in Layers A and B, respectively; and σ_A and σ_B are the geometric standard deviations of the particle distributions of Layers A and B.

It is worth noting that for a system with log-normal size distribution the average particle size is a little bit different from the median particle size. The average particle size, \bar{d}_A and \bar{d}_B , in each layer can be calculated by the following equations [14]:

$$\bar{d}_A = \exp(\ln d_A + 0.5 \ln^2 \sigma_A) \quad (11)$$

and

$$\bar{d}_B = \exp(\ln d_B + 0.5 \ln^2 \sigma_B). \quad (12)$$

The number of particles with the size of d_i in Layer A or d_j in Layer B can thus be calculated as

$$N_i = N_A [f(d_i, d_A, \sigma_A) / \sum f(d_i, d_A, \sigma_A)] \quad (13)$$

and

$$N_j = N_B [f(d_j, d_B, \sigma_B) / \sum f(d_j, d_B, \sigma_B)] \quad (14)$$

where N_A and N_B are the total number of particles in Layers A and B, respectively.

The relationship between the volume, V , and the size, d , of a particle is

$$V = cd^3 \quad (15)$$

where c is a shape factor equal to $\pi/6$ for spherical shape and 1 for cubic shape. Since the value of c have no effect on the final value of n that we are concerned with in this discussion, $c = 0.8$ is chosen. Thus, the total volume of the solid phase in Layer A or Layer B can be obtained as

$$(V_s)_A = \sum cd_i^3 N_i \quad (16)$$

and

$$(V_s)_B = \sum cd_j^3 N_j. \quad (17)$$

Suppose that the two layers are equilibrated under the same liquid migration pressure, P_m , and that $n = 1$, i.e., that the equation suggested by Lisovsky's model [7] of mono-sized WC–Co system holds true for any particle size, then the liquid volume fraction surrounding a WC particle with a size of d_i in Layer A or d_j in Layer B can be calculated from

$$P_m = k_0[(1/u_i - 1)^{1/3} - 1.41u_i]/d_i \quad (18)$$

or

$$P_m = k_0[(1/u_j - 1)^{1/3} - 1.41u_j]/d_j. \quad (19)$$

Thus, the volume of liquid phase surrounding a WC particle with size of d_i in Layer A or d_j in Layer B is, respectively,

$$(V_l)_i = \frac{u_i}{1 - u_i} cd_i^3 \quad (20)$$

or

$$(V_l)_j = \frac{u_j}{1 - u_j} cd_j^3. \quad (21)$$

The total volume of the liquid phase in Layer A or Layer B can thus be obtained:

$$(V_l)_A = \sum \frac{u_i}{1 - u_i} cd_i^3 N_i \quad (22)$$

or

$$(V_l)_B = \sum \frac{u_j}{1 - u_j} cd_j^3 N_j \quad (23)$$

The average values of liquid volume fraction in Layer A or Layer B can thus be obtained, respectively, as

$$u_A = (V_l)_A / [(V_l)_A + (V_s)_A] \quad (24)$$

or

$$u_B = (V_l)_B / [(V_l)_B + (V_s)_B] \quad (25)$$

Since the average particle sizes and liquid volume fractions in Layer A and Layer B are \bar{d}_A and \bar{d}_B , and u_A and u_B , respectively, the apparent value of n can be calculated based on the following equation from Eq. (4):

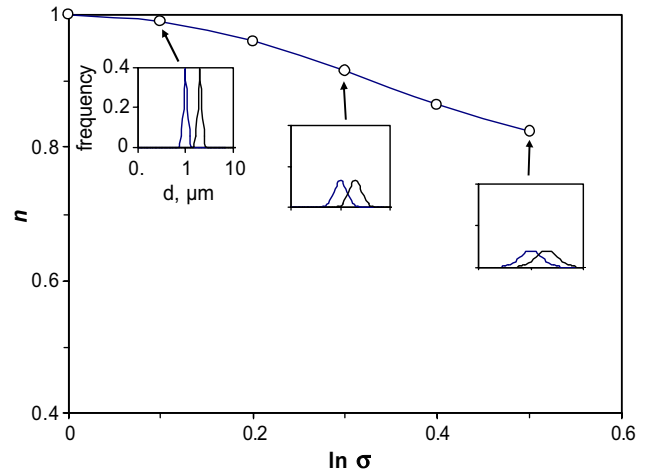


Fig. 4. Decrease in n value with increasing width of particle size distribution. σ is the geometric standard deviation of particle size distribution for both layers, i.e. $\sigma = \sigma_A = \sigma_B$. $n = 1$ was assumed for the WC–Co with mono-sized WC particles. The three imbedded small figures demonstrate the width of particle size distributions.

$$n = \frac{\ln\{[(1/u_A - 1)^{1/3} - 1.41u_A] / [(1/u_B - 1)^{1/3} - 1.41u_B]\}}{\ln(\bar{d}_A/\bar{d}_B)} \quad (26)$$

In order to examine the effect of particle size distribution on the average value of n , the average values of n have been calculated for constant values of $P_m = 0.5$ MPa, $d_A = 1$ μm , $d_B = 2$ μm , but with different values of the geometric standard deviation. As shown in Fig. 4, the apparent value of n decreases with the increasing width of the particle size distribution.

If $n = 1$ was true for mono-sized WC particles, the standard deviation of the particle size distribution would have been unreasonably large in order to obtain the observed small n value of 0.4, according to Fig. 4. However, $n = 1$ was postulated for mono-sized and isometric-shaped particles, it is thus expected that we will find $n \neq 1$ (quite probably $n < 1$) even for mono-sized WC particles, since WC particles are not isometric in shape. Due to mathematical complexities in examining the effect of non-isometry in particle shape, it is beyond the scope of this article to find the small n value for mono-sized WC particles. Though it is uncertain now how small the n value will be for mono-sized WC particles, the observed small n value for real WC–Co composite should result from the WC particle size distribution and the non-isometric WC particle shape.

6. Conclusions

The driving force of liquid phase migration or liquid redistribution during liquid phase sintering is liquid migration pressure, which is dependent on two primary factors in real composite materials: the liquid volume fraction and the solid particle size. In this study, the effect of solid particle size on liquid migration pressure has been studied

experimentally for the WC–Co system, and thus the dependence of liquid migration pressure on both the volume fraction of liquid Co phase and the WC particle size has been quantitatively established, enabling the prediction of the final Co composition gradient in liquid-phase-sintered WC–Co composite. This result is expected to be valuable in design and manufacture of functionally graded WC–Co composite materials.

References

- [1] Lisovsky AF. On the imbibition of metal melts by sintered carbides. *Powder Metall Int* 1987;19:18–21.
- [2] Lisovsky AF. The migration of metal melts in sintered composite materials. *Int J Heat Mass Transfer* 1990;33:1599–603.
- [3] Eso O, Fang Z, Griffo A. Liquid phase sintering of functionally graded WC–Co composites. *Int J Refractory Met Hard Mater* 2005;23:233–41.
- [4] Beere W. A unifying theory of the stability of penetrating liquid phases and sintering pores. *Acta Metall* 1975;23:131–8.
- [5] Park HH, Yoon DN. Effect of dihedral angle on the morphology of grains in a matrix phase. *Metall Trans A* 1985;16:923–8.
- [6] Delannay F, Pardoën D, Colin C. Equilibrium distribution of liquid during liquid sintering of composition gradient materials. *Acta Mater* 2005;53:1655–64.
- [7] Lisovsky AF. Migration of metal melts in sintered composite bodies. Kiev: Naukova Dumka; 1984.
- [8] Lisovsky AF. Mass transfer of liquid phase in sintered composite materials when interacting with metal melts. *Int J Refractory Met Hard Mater* 1989;8:133–6.
- [9] Suresh S, Mortensen A. Fundamentals of functionally graded materials. London: The Institute of Materials; 1998. p. 28.
- [10] Eso O. PhD dissertation, University of Utah, November; 2006.
- [11] Mahale AE. Phase diagrams for ceramists, vol. X. American Ceramic Society; 1994.
- [12] Uhrenius B. Evaluation of molar volumes in the Co–W–C system and calculation of volume fractions of phases in cemented carbides. *Int J Refractory Met Hard Mater* 1993–1994;12:121–7.
- [13] Exner HE, Fischmeister H. Structure of sintered tungsten carbide–cobalt alloys. *Arch Eisen* 1966;37:417–26.
- [14] DeHoff RT, Rhines FN. Quantitative microscopy. New York: McGraw-Hill; 1968. p. 29.